Structure and Mechanism of Action of the Antimicrobial Peptide Piscidin

Sylvie Campagna, Nathalie Saint, Gérard Molle,* and André Aumelas

CNRS UMR5048, Centre de Biochimie Structurale, F34090 Montpellier, France, INSERM U554, F34090 Montpellier, France, and Université Montpellier 1 et 2, F34090 Montpellier, France

Received September 29, 2006; Revised Manuscript Received December 7, 2006

ABSTRACT: Piscidin, an antibacterial peptide isolated from the mast cells of striped bass, has potent antimicrobial activity against a broad spectrum of pathogens in vitro. We investigated the mechanism of action of this 22-residue cationic peptide by carrying out structural studies and electrophysiological experiments in lipid bilayers. Circular dichroism experiments showed that piscidin was unstructured in water but had a high α-helix content in dodecylphosphocholine (DPC) micelles. ^{1}H NMR data in water and TFE confirmed these results and demonstrated that the segment of residues 8−17 adopted an α-helical structure in a micellar environment. This molecule has a marked amphipathic character, due to well-defined hydrophobic and hydrophilic sectors. This structure is similar to those determined for other cationic peptides involved in permeabilization of the bacterial membrane. Multichannel experiments with piscidin incorporated into azolectin planar bilayers gave reproducible *I*−*V* curves at various peptide concentrations and unambiguously showed that this peptide permeabilized the membrane. This pore forming activity was confirmed by single-channel experiments, with well-defined ion channels obtained at different voltages. The characteristics of the ion channels (voltage dependence, only one or two states of conductance) clearly suggest that piscidin is more likely to permeabilize the membrane by toroidal pore formation rather than via the "barrel-stave" mechanism.

Antibacterial peptides play an important role in the innate immune response to bacterial challenge and thus in ensuring the first-line defenses of many species (*1*, *2*). These peptides are frequently α-helical (*3*), with several positive charges and an amphipathic character. These features seem to play an essential role in the various mechanisms of membrane permeabilization, which often lead to cell death (*4*−*7*).

Several models of membrane permeabilization mechanisms have been developed. In the "barrel-stave" model, the membrane is permeabilized by the formation of transmembrane pores composed of a bundle of α-helices, as described for alamethicin, ceratotoxins, and distinctin (*8*−*11*). In the toroidal pore model, as proposed for magainin (*12*, *13*), lipids are inserted between helices to form a mixed pore. In a third model, the "carpet-like" mechanism, peptides act as a detergent, disrupting the bacterial membrane by forming eventually transitory pores (*14*). In all these models, the physical properties of the helices (charge, length, amphipathicity, etc.) are key elements of the mechanisms operating at various stages, at the surface of the membrane, within the membrane, or both. The complex lipidic composition of the membrane bacteria as well as the total charge of the lipid headgroups also plays an important role in the mechanisms of action of antibacterial peptides.

Besides these pore forming mechanisms, several observations suggest that these antimicrobial peptides can also inhibit the synthesis of the cell wall, nucleic acids, and proteins or even inhibit enzymatic activity (*7*).

Piscidins were the first antimicrobial cationic peptides to be isolated from the mast cells of striped bass (*15*, *16*). Piscidin-1 (Arg^{18}) and piscidin-2 (Lys^{18}) were also discovered in the skin and gills of the striped bass at approximately the same time and named sb- and wb-moronecidins, respectively (*17*). These 22-residue peptides have broad-spectrum activity against bacteria, fungi, and viruses and moderate hemolytic activity. MIC[1] values determined against *Staphylococcus aureus* for piscidin-1 (or sb-moronecidin), piscidin-2 (or wb-moronecidin), and piscidin-3 are 3.1, 1.25−2.5, and 3.1 μM, respectively (*15*, *17*). Piscidin-2 was not hemolytic for human and sheep erythrocytes at concentrations of <2.5 μM (*17*). They are very similar to other antimicrobial peptides from fish (see Figure 1), such as dicentracin from labrax (*18*), epinecidin-1 from grouper (*19*), chrysophsins from bream (*20*), and pleurocidin-like peptides from flounder (*21*). Preliminary circular dichroism (CD) studies showed that piscidins (or moronecidins) and chrysophsins were unstructured in water but had a strong α-helical structure when TFE was added. The Shiffer-Edmundson helical wheel diagram indicated a probable amphipathic α-helical structure (*15*, *17*). This diagram showed two well-defined hydrophilic and hydrophobic sectors, characteristic of a strongly amphipathic molecule. To study the mechanism of action of the piscidin-1

* To whom correspondence should be addressed. Telephone: 33 4 67 41 79 12. Fax: 33 4 67 41 79 13. E-mail: molle@cbs.cnrs.fr.

[1] Abbreviations: AMP, antimicrobial peptide; CD, circular dichroism; CSI, chemical shift index; DPC, perdeuterated dodecylphosphocholine; DQF-COSY, two-dimensional double-quantum-filtered correlated spectroscopy; MIC, minimum inhibitory concentration; NMR, nuclear magnetic resonance; NOE, nuclear Overhauser effect; NOESY, two-dimensional nuclear Overhauser effect spectroscopy; rmsd, root-mean-square deviation; TOCSY, total correlation spectroscopy; TFE, 2,2,2-trifluoroethanol; TPPI, time-proportional phase incrementation.

10.1021/bi0620297 CCC: $37.00
Published on Web 01/25/2007

Peptide	Sequence	Similarities (%)
Piscidin-1	FFHHIFRGIVHVGKTIHRLVTG	100
Moronecidin precursor(1)	FFHHIFRGIVHVGKTIHRLVTG	100
Moronecidin precursor(2)	FFHHIFRGIVHVGKTIHKLVTG	95
Piscidin-2	FFHHIFRGIVHVGKTIHKLVTG	95
Moronecidin precursor(3)	FFHHIFKGIVHVGKTIHRLVTG	95
Dicentracin precursor	FFHHIFRGIVHVGKSIHKLVTG	91
Piscidin-3	FIHHIFRGIVHAGRSIGRFLTG	68
Epinecidin	FIFHIIKGLFHAGKMIHGLVT	57
Chrysophsin-2	FFGWLIRGAIHAGKAIHGLI	50
Chrysophsin-1	FFGWLIKGAIHAGKAIHGLI	45
Pleurocidin-like peptide	FLGLLFHGVHHVGKWIHGLIHG	45

FIGURE 1: Sequence alignment of peptides or protein fragments that exhibit significant levels of identity in sequence to piscidin. The sequences and the alignment were obtained with FASTA3 at the EMBL-EBI, using the Uniprot database (http://www.embl-heidelberg.de/). Conserved residues are colored black, and residues conserved in all sequences are shown in bold. Note that the moronecidin-1 and -2 sequences are identical to the piscidin-1 and -2 sequences, respectively: sb-moronecidin precursor, Q8UUG2 moronecidin precursor, P59906 dicentracin precursor, Q2VWH5 moronecidin, P0C006 piscidin-3, Q6JWQ9 epinecidin, P83546 chrysophsin-2, P83545 chrysophsin-1, and Q7SZG6 pleurocidin-like peptide.

amidated isoform, we carried out multichannel and single-channel experiments in bilayers of azolectin. This mixture of lipids presents a percentage of negatively charged lipids (20%) similar to the one found in outer membranes of Gram-negative bacteria (*22*). In parallel, we determined its three-dimensional structure via NMR experiments in different environments, including dodecylphosphocholine (DPC) micelles that provide a zwitterionic lipid surface similar to that of the membrane (*23*, *24*).

MATERIALS AND METHODS

Chemicals. Piscidin (FFHHIFRGIVHVGKTIHRLVTG-NH_2; M_w = 2571 Da; pI ≈ 12) was generously provided by E. J. Noga (Raleigh, NC). Soybean azolectin IV-S was purchased from Sigma. ($^2H_{38}$)DodPCho dodecylphosphocholine (DPC; M_w = 389.5 Da) was purchased from EURISOTOP.

Circular Dichroism Measurements. CD spectra were recorded at room temperature on a Chirascan dichrograph (Applied Photophysics) in a quartz cell with an optical path of 0.5 mm for peptides in aqueous solution. Five scans were performed, and band positions were determined after smoothing the spectra using the Savitzky−Golay method. The peptide concentration was 1.25×10^{-4} M in 20 mM sodium phosphate (pH 7.4). In the experiment performed in 1% DPC (25 mM), the DPC/peptide molar ratio was ∼200. The percentage of the various secondary structures was calculated with DICHROWEB (*25*).

Conductance Experiments. In macroscopic and single-channel conductance experiments, virtually solvent-free planar lipid bilayers were formed by the Montal and Mueller technique (*26*). The membrane was formed over a 100−150 μm hole in a Teflon film (10 μm thick), which had been treated with a 1:40 mixture (v/v) of hexadecane and hexane, separating two glass half-cells. After 2 h, 10 μL of an azolectin/hexane solution (5:1000) was added to both sides of the cell containing 2 mL of electrolyte solution [1 M KCl, 10 mM *N*-(2-hydroxyethyl)piperazine-*N*′-2-ethanesulfonic acid (HEPES) (pH 7.4)]. Bilayers were formed by lowering and increasing the level of electrolyte in one or both sides and monitoring capacitance responses. Voltage was applied through an Ag/AgCl electrode on the cis side. The peptide was added to both compartments, typically at 10^{-11}−10^{-10} M for single-channel experiments and 10^{-8}−10^{-7} M for macroscopic measurements.

In macroscopic conductance experiments, the doped membranes were subjected to slow voltage ramps (10 mV/s) and transmembrane currents were fed into an amplifier (BBA-01, Eastern Scientific, Rockville, MD). Current−voltage curves were stored on a computer and analyzed with Scope (Bio-Logic, Claix, France).

In single-channel recordings, currents were amplified and potentials applied simultaneously with a patch-clamp amplifier (RK 300, Bio-Logic). Single-channel currents were monitored using an oscilloscope (TDS 3012, Tektronix, Beaverton, OR), filtered at 300 Hz, and stored on a CD recorder (DRA 200, Bio-Logic) for offline analysis. Data were analyzed with Windac32 (http://www.shareit.com) and Biotools (Bio-Logic). All experiments were performed at room temperature.

NMR Spectroscopy. Samples of piscidin for NMR were prepared in a 95:5 (v/v) mixture of H_2O and D_2O to yield

0.8−1.0 mM solutions. The pH was adjusted to the desired value by adding DCl or NaOD and was checked at room temperature with a 3 mm electrode. The pH values given have not been corrected for the deuterium isotopic effect. Proton chemical shifts are expressed with respect to sodium 4,4-dimethyl-4-silapentane-1-sulfonate, according to the IUPAC recommendations. We carried out ^{1}H NMR experiments on a Bruker Avance 600 spectrometer equipped with a triple-resonance cryoprobe, and spectra were recorded at temperatures ranging from 15 to 42 °C. In all experiments, the carrier frequency was set at the center of the spectrum, at the frequency of water. Spectra produced by double-quantum-filtered correlated spectroscopy (DQF-COSY) (*27*, *28*), z-filtered total correlated spectroscopy (z-TOCSY) (*29*, *30*), and nuclear Overhauser effect spectroscopy (NOESY) (*31*) were acquired in the phase-sensitive mode, using the States−TPPI method (*32*). For spectra recorded in H_2O, the resonance of the water was suppressed by the WATERGATE method (*33*), except for DQF-COSY spectra, for which low-power irradiation was used. We obtained z-TOCSY spectra with a mixing time of 90 ms and NOESY spectra with mixing times of 100, 150, and 300 ms. Data were processed with XWINNMR. Full sequential assignment was achieved using the general strategy described by Wüthrich (*34*).

Piscidin studies in the presence of trifluoroethanol were carried out with 25 and 50% trifluoroethanol (v/v).

Finally, another 1 mM sample was used to study the solution structure of piscidin in a micellar environment. We added DPC gradually (2.5 mg at a time) until 12.5 mg had been added (DPC:peptide molar ratio of 64). After each addition, DQF-COSY, TOCSY (isotropic mixing time of 70 ms), and NOESY (mixing time of 200 ms) spectra were recorded.

Calculation of Structures. NMR-derived constraints measured on NOESY spectra were converted into interproton upper distance limits of 2.5, 3.0, 4.0, and 5.0 Å for strong, medium, weak, and very weak intensities, respectively. Lower distance limits were taken as the sum of the van der Waals radii. As no stereospecific assignment was possible for the methyl and methylene protons, pseudoatoms were used instead, after appropriate corrections of the constraints.

The ϕ angle restraints were estimated from the $^3J_{NH-CH}$ coupling constants and the χ_1 angle restraints were derived from the combined analysis of the $^3J_{H\alpha-H\beta\beta'}$ coupling constants and intraresidue NOEs. For the calculation of three-dimensional structures, distance and dihedral angle restraints were input into DYANA, a program using simulated annealing combined with molecular dynamics in torsion angle space (*35*). In the first stage of the calculation, an initial set of 20 structures was generated from a template structure with randomized Ψ and Φ dihedral angles and extended side chains. In preliminary calculations, hydrogen bonds were not used as a restraint. Hydrogen bonds were considered to be present if the distance between heavy atoms was less than 3.5 Å and the donor−hydrogen−acceptor angle was greater than 120°. Finally, we used 167 NOE-derived distances and nine dihedral constraints to calculate the structure of piscidin in the presence of DPC micelles. Calculations were made for 60 conformers, and the resulting 10 structures with minimal restraint violations (no violation of >0.3 Å) were analyzed with INSIGHT 97 (Molecular Simulation Inc., San Diego, CA). Ramachandran analysis was performed with PROCHECK (*36*). The limits of the secondary structure elements and the van der Waals surfaces and accessible surface area for each residue were determined with STRIDE (*37*). The chemical shifts and NMR-derived constraints are deposited in the BRMB (accession number 15050). Coordinates of piscidin are available on request (andre.aumelas@cbs.cnrs.fr).

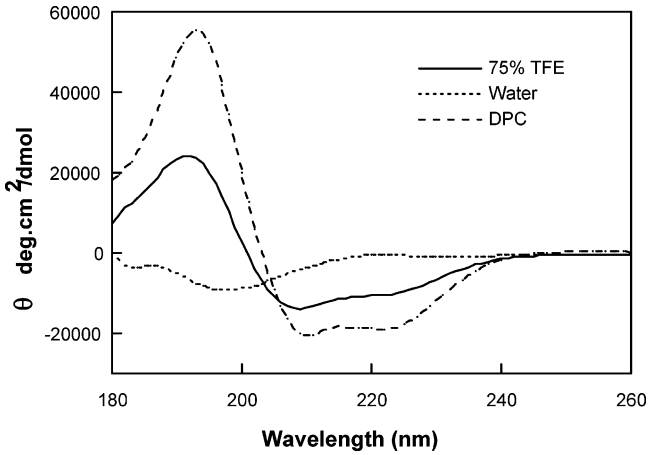

FIGURE 2: Circular dichroism spectra for piscidin. The spectra were obtained in water, with 10−75% TFE and 1% DPC [buffered with 10 mM sodium phosphate (pH 7.4)]. For spectra recorded in the presence of TFE, only that with 75% is displayed. The peptide concentration was 1.25×10^{-4} M. Five scans were recorded at room temperature.

RESULTS

Circular Dichroism Study

CD spectra were recorded in various solutions buffered with 20 mM sodium phosphate at pH 7.4 (Figure 2). In water, a typical random coil spectrum was obtained. In 75% TFE, a standard α-helix signal was detected, with characteristic bands at 195, 208, and 222 nM. A more accentuated α-helical conformation was observed in the presence of 1% DPC (lipid:peptide molar ratio of 200). Indeed, the percentage of α-helix in DPC micelles was ∼65%, whereas that in 75% TFE was only 40%.

Ion Channel Formation

Macroscopic Current Measurements. Piscidin was incorporated into azolectin planar lipid bilayers formed by the Montal−Mueller technique (*26*). Typically, after 30 min (the time required to stabilize the membrane), the bilayer was subjected to repetitive triangular ramping (10 mV/s). $I-V$ curves were obtained at various concentrations of piscidin in 1 M KCl (Figure 3). The development of exponential branches occurred above a voltage threshold (V_c) depending on the peptide concentration (*38*). Differences in V_c values made it possible to estimate concentration dependence (V_a), which is the shift of V_c produced by an e-fold change in peptide concentration. The V_a value of 52 ± 5 mV obtained for piscidin is indicative of strong concentration dependence. Finally, the voltage increment (V_e) resulting in an e-fold change in conductance on the exponential branch gave a value of 24 ± 2 mV, characteristic of weak voltage dependence, in contrast to the value of 6 mV obtained for alamethicin (*38*). Thus, the V_a/V_e ratio, known as N_{app} (*38*), the apparent number of monomers constituting the pore-

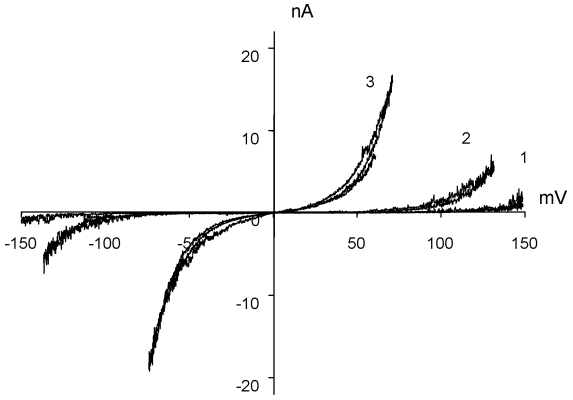

FIGURE 3: Macroscopic current−voltage curves ($I-V$) for piscidin at different concentrations in azolectin membranes. $I-V$ curves between −150 and 150 mV, at a ramp sweep of 10 mV/s in 1 M KCl. Peptide concentrations were 3×10^{-8} (curve 1), 10^{-7} (curve 2), and 3.5×10^{-7} M (curve 3).

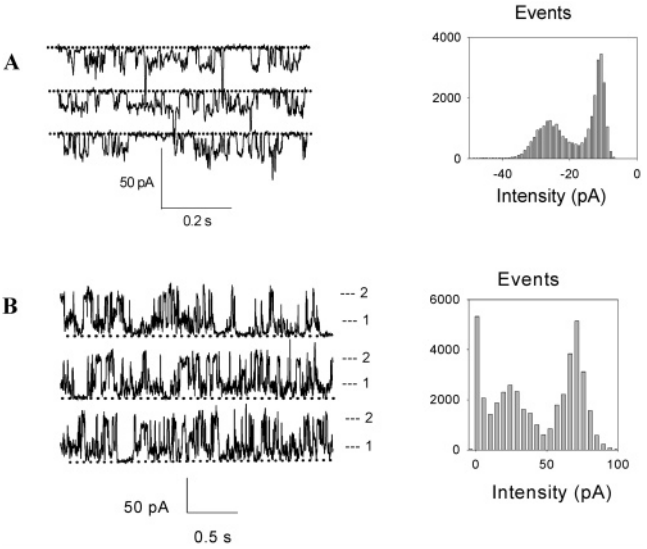

FIGURE 4: Single-channel recordings for piscidin in 1 M KCl and the associated amplitude histograms (A) at −80 mV and (B) at 100 mV. The piscidin concentration was 5×10^{-9} M. The closed state is represented by a dotted horizontal line. The conductance of channels was calculated from the difference between the closed state and the open states divided by the applied voltage value.

forming aggregate according to the barrel-stave model, was not significant (we obtained a value of 2.1 ± 0.4). This mechanism is characterized by values above 4.

Single-Channel Recordings. We also studied channel formation by piscidin by means of single-channel conductance measurements, after incorporating the peptide into planar lipid bilayers, using the technique described above. Piscidin formed ion-permeable channels at all applied voltages between −150 and 150 mV. Rapid, discrete current fluctuations occurred at −80 mV (Figure 4A). The associated amplitude histogram gave a conductance value of 200 pS in 1 M KCl. Other levels of conductance were occasionally recorded in other experiments. The trace in Figure 4B shows the conductance level of 200 pS previously recorded and another level of conductance at 720 pS. This behavior differs from that of alamethicin, the archetype of the barrel-stave model, because piscidin did not induce a typical multistate behavior. In the barrel-stave model, the fluctuations between substates are correlated with the uptake or release of monomers by the conducting bundle, and the different subconductance levels are characterized by nonintegral increments.

NMR Structural Study

In the ^{1}H NMR spectrum of piscidin recorded in water at 22 °C and pH 5.0, most of the amide signals are in the 8.8−8.1 ppm range (except that of Gly^8, 7.58 ppm), suggesting that the peptide is mainly unstructured in water (Figure 5). In NOESY experiments, sequential NOEs of strong intensity facilitated the identification and assignment of all the spin systems. Four NN NOEs of weak intensity (Phe^6−Arg^7, Arg^7−Gly^8, Gly^8−Ile^9, and His^{11}−Val^{12}) were also observed. The Phe^6−Ile^9 consecutive NOEs indicate that this sequence tends to adopt a poorly stable helical structure in water. Overall, the absence of medium- and long-range NOEs indicates that piscidin is essentially unstructured in water.

The addition of 25% TFE had no significant overall effect on the ^{1}H NMR spectrum. However, there was a significant and global upfield shift of amide signals of ∼0.25−0.30 ppm. In addition, the methyl signals of Thr^{15} (1.15 ppm) and Thr^{21} (1.24 ppm), which were well-separated in water, overlapped in the presence of TFE. The NOESY spectrum exhibited more NN NOEs than in water, indicating the presence of a significant percentage of helical structure (data not shown). The addition of TFE to a concentration of 50% slightly increased the degree of dispersion of amide and methyl signals and led to line broadening, particularly for amide signals. The NOESY spectrum exhibited several successive NN NOEs of strong intensity, indicating the formation of a more stable helical structure (data not shown). These results were confirmed by a similar study performed by CD measurements in the presence of 10−75% TFE (Figure 2). Above 40−50% TFE, the CD spectrum remained very similar, indicating that there are no significant conformational changes for higher percentages of TFE.

Piscidin is thought to act at a membrane level. We therefore carried out a structural study in the presence of DPC, a zwitterionic lipid. Such a micellar environment is considered to mimic the amphipathic environment of a phospholipid bilayer and the bilayer−water interface (*24*). We recorded an initial set of spectra for different concentrations of DPC and then determined the structure of piscidin in interaction with micelles.

The addition of 13 equiv of DPC (∼13 mM) induced line broadening. The effects of DPC on chemical shifts reached a plateau at around 39−64 equiv (∼39−64 mM). Amide resonances in the 8.9−7.7 ppm range were more disperse than in water, suggesting a more constrained conformation. These spectral changes indicated an interaction between piscidin and the DPC micelles giving rise to a more constrained structure.

Full assignment was achieved with three data sets, corresponding to COSY, TOCSY, and NOESY experiments carried out at pH 5 and at 27, 37, and 42 °C, respectively. Then, chemical shifts of α-protons sensitive to conformational changes were analyzed, and NMR-derived constraints were used to determine the conformation of piscidin that binds to DPC micelles.

The chemical shifts of the α-protons measured in the presence of DPC micelles (DPC:peptide molar ratio of 39)

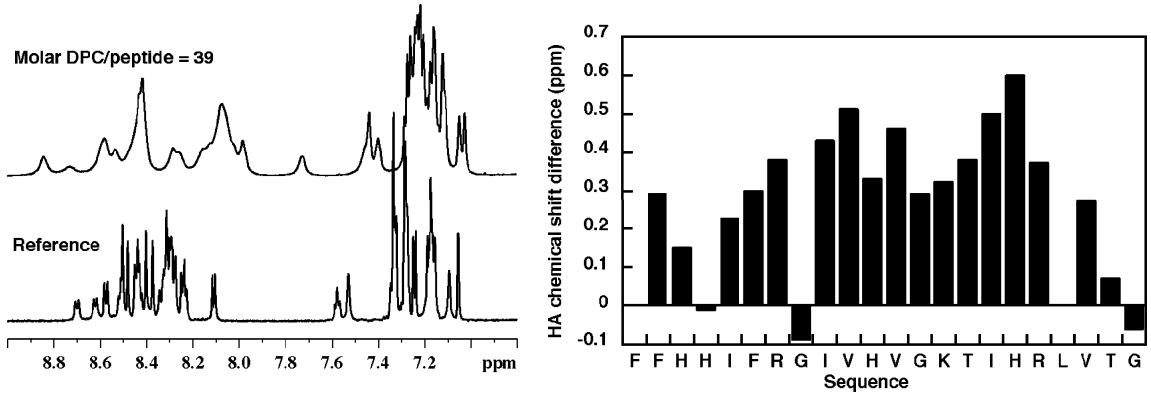

FIGURE 5: Changes in the piscidin ^{1}H NMR spectrum and chemical shift differences for α-protons upon addition of DPC (molar DPC: peptide ratio of 39 at 27 °C). For glycine, the chemical shift was calculated from the downfield-shifted resonance.

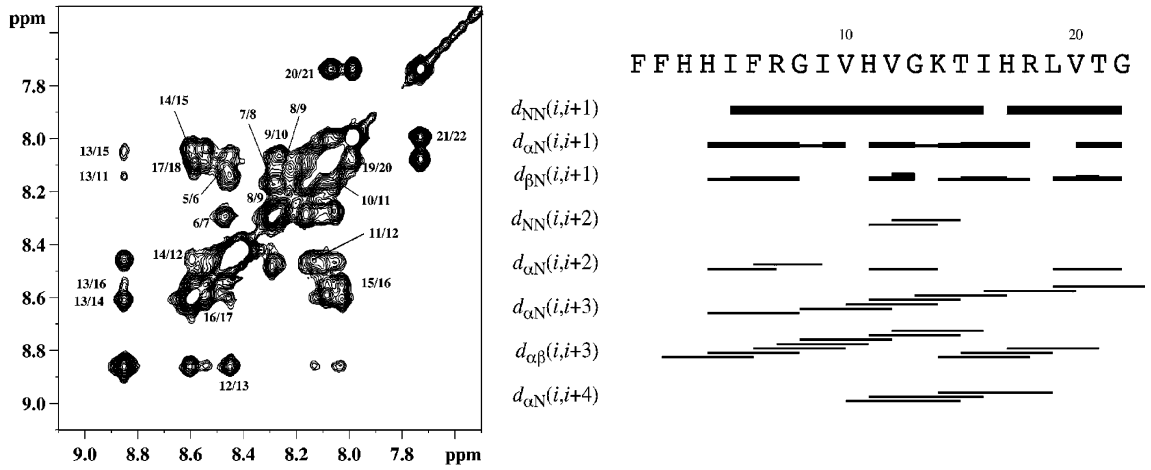

FIGURE 6: Part of the NOESY map showing the NN dipolar interactions and chart of the NOEs measured for piscidin interacting with DPC micelles (molar DPC:peptide ratio of 39 at 27 °C with a mixing time of 200 ms).

were compared with those measured in water, in which piscidin adopts an unstructured conformation (Figure 5). This comparison revealed that, with the exception of Gly[8] and Leu[19], most α-proton resonances spanning 5−20 residues displayed marked upfield shifts in the 0.2−0.6 ppm range, suggesting the formation of an α-helical structure during interactions with DPC micelles. Similar chemical shift differences were obtained when compared with statistic values for a random coil structure (*39*, *40*) (data not shown). The helical structure was confirmed by the numerous successive and strong NN and $\alpha_i-\beta_{i+3}$ NOEs that were observed (Figure 6).

We used a set of 176 NMR-derived constraints (167 distance constraints and nine angle constraints) to calculate the structure of piscidin bound to micelles. A stereoview of a family of 10 conformers is displayed in Figure 7. The superimposition of all these conformers resulted in an average rmsd of 1.41 ± 0.33 Å. The well-defined part of the molecule (residues 6−21), with an average rmsd of 0.33 ± 0.12 Å, contrasts with the less well-defined N-terminal part of the molecule (residues 1−5). The Ramachandran plot indicated that 98.3% of the residues were in the most favored and additional allowed regions, 1.1% were in the generously allowed region, and 0.6% was in the disallowed region (His[3] for one conformer). The limits of the secondary structure elements indicated that the structure of piscidin comprised a helical portion (residues 8−17) and three β-turns: a type IV β-turn spanning residues 2−5 and two type I β-turns spanning residues 17−20 and 19−22.

As a result, in the presence of DPC micelles, piscidin mainly adopts an α-helical structure and thus belongs to the α-helical class of antimicrobial peptides.

The average surface area of the micelle-bonded conformers was 2590 Å^2. The hydrophobic side chains included Phe[1], Phe[2], Ile[5], Phe[6], Ile[9], Val[10], Val[12], Ile[16], Leu[19], and Val[20], and the hydrophilic side chains included His[3], His[4], Arg[7], His[11], Lys[14], Thr[15], His[17], Arg[18], and Thr[21]. The mean hydrophobic and hydrophilic areas were 1298 (50.1%) and 1292 Å^2 (49.9%), respectively. The hydrophobic and hydrophilic equivalent surface areas are responsible for the strongly amphipathic character of piscidin.

DISCUSSION

Piscidin, a 22-residue cationic peptide isolated from the mast cells or gills of bass (*15*, *17*), has antimicrobial activity, possibly due to its ability to permeabilize bacterial membranes. As in many antimicrobial peptides, both the number of positively charged residues (two arginines, one lysine, and four histidines) and the ability to form an amphipathic helical structure in membrane-mimicking environments seem to be the two main features responsible for the antimicrobial activity of piscidin.

Many antimicrobial peptides adopt a helical structure upon interaction with DPC micelles. This has been shown to be

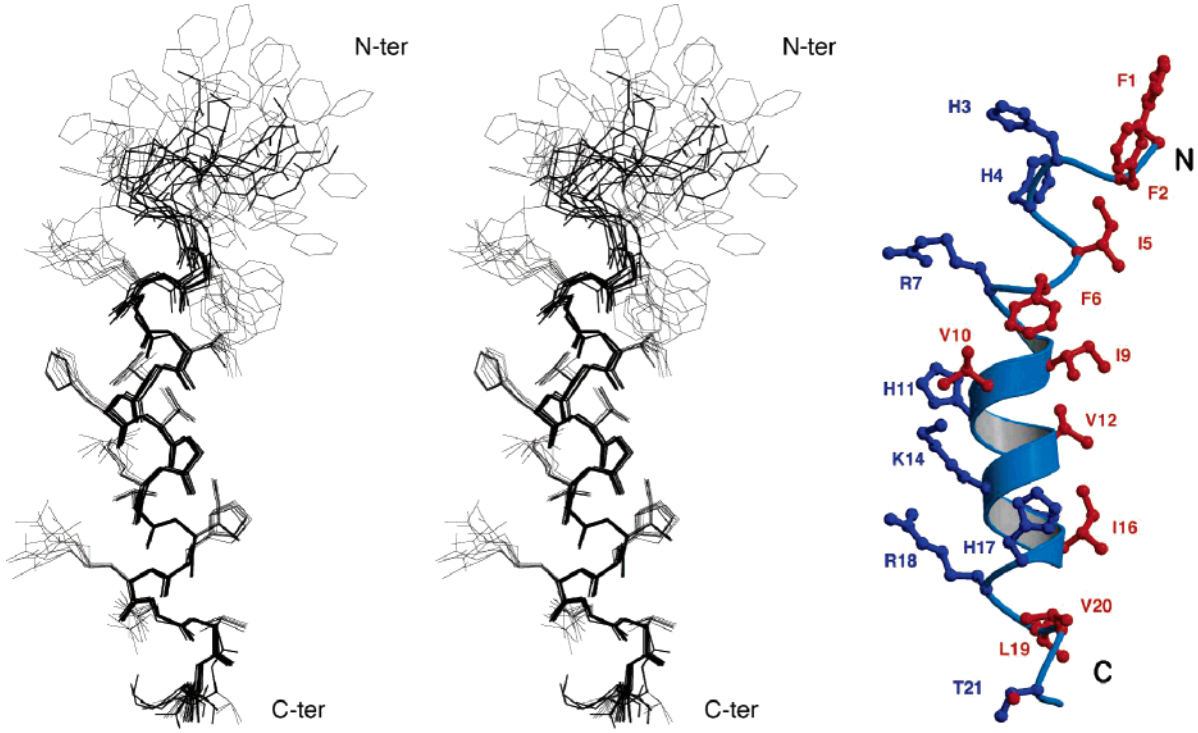

FIGURE 7: Stereoview of a family of 10 piscidin conformers bound to DPC micelles. The amphipathic feature of the structure is highlighted on the Molscript structure (*57*). Hydrophilic and hydrophobic side chains are colored blue and orange, respectively. The hydrophobic area is thought to be part of the piscidin−micelle interface. In contrast, the hydrophilic side chains are thought to be exposed to the solvent.

the case for bacteriocin (*41*), melittin (*42*), PMAP-23 (*43*), zervamicin (*44*), sakacin (*45*), pleurocidin (*46*), CRAMP (*47*), SMAP-29 (*48*), and ranalexin (*49*). Circular dichroism experiments carried out with piscidin at pH 7.4 showed that this peptide adopts a random coil structure in water and an α-helical structure (40%) in 75% TFE. The α-helix content of the molecule was significantly higher (65%) in the presence of DPC micelles. This change in conformation suggests that the helical structure is probably the active conformation able to permeabilize the membrane.

NMR experiments were performed in various media, to determine the three-dimensional structure of piscidin. This molecule was mainly unstructured in water. As shown by CD and NMR experiments, the addition of TFE led to the formation of a helical structure. In a DPC micellar environment, piscidin interacted with micelles and its sequence of residues 8−17 adopted an α-helical structure. Interestingly, a similar induced conformational change has been reported for pleurocidin, a 25-residue antimicrobial peptide (*46*). In a recent solid-state NMR study of piscidin in the presence of hydrated oriented lipid bilayers, piscidin was also found to adopt an α-helical structure, lying parallel to the membrane surface (*50*). The overall structure of piscidin was markedly amphipathic, with hydrophobic and hydrophilic sectors comparable in size. CD and NMR piscidin data were collected in salt-free media. However, it should be noticed that in the presence of 160−1280 mM NaCl, the MIC value was doubled for wb-moronecidin (piscidin-2) against *S. aureus* (*17*). In the presence of high concentrations of salt, cations can interact with negative charges of the membrane and compete with the peptide−membrane electrostatic interactions. Thus, we have to be aware of possible alterations of AMP solubility, antimicrobial activity, and to a lesser extent conformation. On the basis of these results in the presence of different lipids, piscidin was found to interact with various membrane-mimicking interfaces, suggesting that its interaction with them is not only electrostatically mediated.

The piscidin sequence contains four histidine residues located on the solvent-exposed side of the amphipathic helix. The pK_a of such a solvated histidine usually is around 6.5. Since all histidine are solvated, their pK_a is probably ≥6.5. For an α-helical peptide of a similar size, the histidine pK_a in the range of 7.7−7.8 was measured (*51*). Accordingly, the number of positive charges displayed by piscidin can move from ≈7 (two Arg residues, one Lys residue, and four His residues) for pH ≤5.0 where histidine side chains are fully protonated to 3 for pH ≥8 where they are deprotonated. At pH 7.4, due to their partial protonation, the charge state probably displays an intermediate value of >3.

Therefore, the presence of several positive charges combined with a clear-cut distribution of hydrophilic and hydrophobic side chains in a linear α-helical structure suggests that piscidin may act against bacteria by forming pores permeabilizing the bacterial membrane as reported for other antimicrobial peptides. We therefore carried out reconstitution experiments, using planar azolectin bilayers to investigate the behavior of piscidin.

Azolectin is a natural mixture of lipids [phosphatidylethanolamine (PE), phosphatidylinositol (PI), phosphatidylcholine (PC), and phosphatidylserine (PS) with 20% net negatively charged headgroups, most of them being PI (*22*)]. This composition is close to that of the outer membrane of bacteria which also presents ∼20% negative lipids (mainly phosphatidylglycerol). Piscidin gave symmetric $I-V$ curves, making it possible to determine V_a and V_e values (*38*). The 52 ± 5 mV V_a value that was obtained indicates a strong concentration dependence, whereas the V_e value of 24 ± 2

mV indicates that piscidin does not induce voltage-dependent channels. This behavior was confirmed by the weak voltage required to induce ion channels, as pore forming activity was observed at voltages below 70 mV. The obtained N_{app} value is not consistent with the barrel-stave mechanism. The single-channel traces observed at different voltages were also inconsistent with this mechanism. Indeed, the barrel-stave model is characterized by the uptake and release of helical peptides in the conducting bundle, which modify the pore size and induce different levels of conductance. In this model, there may be more than 10 levels, with a geometric progression of increments between levels (*52*). With piscidin, we observed only one level of conductance in most experiments, with two in rare instances. Similar behavior, with a single level of conductance, has previously been reported for magainin (*53*) and pleurocidin (*54*). Another common feature of magainin, pleurocidin, and piscidin is their strong amphipathic character, with a 140−180° positively charged hydrophilic sector on the planar projection of the helical wheel. In contrast, alamethicin has a narrow and uncharged polar sector (<50°), which forms a hydrophilic pore following the association of several monomers via strong hydrophobic interactions. This amphipathic character is an important feature, accounting for the self-association of peptides before their insertion in lipid bilayers. In reconstitution experiments with various amphiphilic α-helical peptides (*10*, *11*, *53*, *54*), we have found that the barrel-stave model is inconsistent with a strongly charged large hydrophilic sector. This hypothesis is supported by several studies. In the first, a study of two synthetic peptides with polar angles of the hydrophilic sector of 100° and 180°, the authors claimed that this factor was an essential determinant of peptide−lipid interactions (*55*). In the second, a study of lysine-containing amphipathic peptides (*56*), the authors concluded that $(LxKy)_n$ polypeptides with a single lysine residue adopted a transmembrane orientation, whereas peptides with two separate lysines in the polar sector were in equilibrium between the planar and transmembrane orientations. Peptides with more than three lysines remained preferentially on the membrane surface. These findings are consistent with solid-state NMR data in the presence of hydrated oriented lipid bilayers (*50*).

On the basis of these arguments, we can exclude the barrel-stave model as a possible mechanism of action of piscidin. The similarities between the pore forming properties of piscidin, pleurocidin, and magainin suggest that the antimicrobial activity of piscidin is due to the formation of toroidal pores in the bacterial membrane. In these pores, the lipids are inserted between the α-helices to form a toroidal hole, so the pore is lined by both the peptides and the lipid head groups.

In conclusion, we have determined the three-dimensional structure of piscidin in various media. In the presence of DPC micelles, this molecule has well-defined hydrophilic and hydrophobic sectors along the practically straight linear molecule, which is mostly α-helical. This conformation, induced during the initial adsorption of the molecule onto the membrane surface, has been reported for many other antimicrobial peptides. When piscidin is incorporated into azolectin bilayers, it displays well-defined single channels at different voltages. The characteristics of these ion channels (voltage dependence, levels of conductance) suggest that piscidin permeabilizes the membrane more likely by toroidal pore formation rather than via the barrel-stave model.

SUPPORTING INFORMATION AVAILABLE

Chemical shifts of piscidin in water (Table 1) and 39 mM DPC (Table 2) at 27 °C. This material is available free of charge via the Internet at http://pubs.acs.org.

REFERENCES

1. Hancock, R. E., and Scott, M. G. (2000) The role of antimicrobial peptides in animal defenses, *Proc. Natl. Acad. Sci. U.S.A. 97*, 8856−8861.
2. Hoffmann, J. A., Kafatos, F. C., Janeway, C. A., and Ezekowitz, R. A. (1999) Phylogenetic perspectives in innate immunity, *Science 284*, 1313−1318.
3. Zasloff, M. (2002) Antimicrobial peptides of multicellular organisms, *Nature 415*, 389−395.
4. Epand, R. M., and Vogel, H. J. (1999) Diversity of antimicrobial peptides and their mechanisms of action, *Biochim. Biophys. Acta 1462*, 11−28.
5. Shai, Y. (2002) Mode of action of membrane active antimicrobial peptides, *Biopolymers 66*, 236−248.
6. Hwang, P. M., and Vogel, H. J. (1998) Structure-function relationships of antimicrobial peptides, *Biochem. Cell Biol. 76*, 235−246.
7. Brogden, K. A. (2005) Antimicrobial peptides: Pore formers or metabolic inhibitors in bacteria? *Nat. Rev. Microbiol. 3*, 238−250.
8. Boheim, G. (1974) Statistical analysis of alamethicin channels in black lipid membranes, *J. Membr. Biol. 19*, 277−303.
9. Baumann, G., and Mueller, P. (1974) A molecular model of membrane excitability, *J. Supramol. Struct. 2*, 538−557.
10. Bessin, Y., Saint, N., Marri, L., Marchini, D., and Molle, G. (2004) Antibacterial activity and pore-forming properties of ceratotoxins: A mechanism of action based on the barrel stave model, *Biochim. Biophys. Acta 1667*, 148−156.
11. Raimondo, D., Andreotti, G., Saint, N., Amodeo, P., Renzone, G., Sanseverino, M., Zocchi, I., Molle, G., Motta, A., and Scaloni, A. (2005) A folding-dependent mechanism of antimicrobial peptide resistance to degradation unveiled by solution structure of distinctin, *Proc. Natl. Acad. Sci. U.S.A. 102*, 6309−6314.
12. Ludtke, S. J., He, K., Heller, W. T., Harroun, T. A., Yang, L., and Huang, H. W. (1996) Membrane pores induced by magainin, *Biochemistry 35*, 13723−13728.
13. Huang, H. W. (2000) Action of antimicrobial peptides: Two-state model, *Biochemistry 39*, 8347−8352.
14. Shai, Y. (1999) Mechanism of the binding, insertion and destabilization of phospholipid bilayer membranes by α-helical antimicrobial and cell non-selective membrane-lytic peptides, *Biochim. Biophys. Acta 1462*, 55−70.
15. Silphaduang, U., and Noga, E. J. (2001) Peptide antibiotics in mast cells of fish, *Nature 414*, 268−269.
16. Chinchar, V. G., Bryan, L., Silphadaung, U., Noga, E., Wade, D., and Rollins-Smith, L. (2004) Inactivation of viruses infecting ectothermic animals by amphibian and piscine antimicrobial peptides, *Virology 323*, 268−275.
17. Lauth, X., Shike, H., Burns, J. C., Westerman, M. E., Ostland, V. E., Carlberg, J. M., Van Olst, J. C., Nizet, V., Taylor, S. W., Shimizu, C., and Bulet, P. (2002) Discovery and characterization of two isoforms of moronecidin, a novel antimicrobial peptide from hybrid striped bass, *J. Biol. Chem. 277*, 5030−5039.
18. Salerno, G. R. P., and Sri Widada, J. (2003) Dicentracine, first antimicrobial peptide isolated from the fish *Dicentrarchus labrax*. Submitted to the EMBL/GenBank/DDBJ databases.
19. Yin, Z. X., He, W., Chen, W. J., Yan, J. H., Yang, J. N., Chan, S. M., and He, J. G. (2006) Cloning, expression and antimicrobial activity of an antimicrobial peptide, epinecidin-1, from the orange-spotted grouper, *Epinephelus coioides*, *Aquaculture 253*, 204−211.
20. Iijima, N., Tanimoto, N., Emoto, Y., Morita, Y., Uematsu, K., Murakami, T., and Nakai, T. (2003) Purification and characterization of three isoforms of chrysophsin, a novel antimicrobial peptidein the gills of the red sea bream, *Chrysophrys major*, *Eur. J. Biochem. 270*, 675−686.

21. Douglas, S. E., Gallant, J. W., Gong, Z., and Hew, C. (2001) Cloning and developmental expression of a family of pleurocidin-like antimicrobial peptides from winter flounder, *Pleuronectes americanus* (Walbaum), *Dev. Comp. Immunol. 25*, 137−147.

22. Donovan, J. J., Simon, M. I., and Montal, M. (1982) Insertion of diphtheria toxin into and across membranes: Role of phosphoinositide asymmetry, *Nature 298*, 669−672.

23. Schievano, E., Calisti, T., Menegazzo, I., Battistutta, R., Peggion, E., Mammi, S., Palu, G., and Loregian, A. (2004) pH-dependent conformational changes and topology of a herpesvirus translocating peptide in a membrane-mimetic environment, *Biochemistry 43*, 9343−9351.

24. Damberg, P., Jarvet, J., and Graslund, A. (2001) Micellar systems as solvents in peptide and protein structure determination, *Methods Enzymol. 339*, 271−285.

25. Lobley, A., Whitmore, L., and Wallace, B. A. (2002) DICHROWEB: An interactive website for the analysis of protein secondary structure from circular dichroism spectra, *Bioinformatics 18*, 211−212.

26. Montal, M., and Mueller, P. (1972) Formation of bimolecular membranes from lipid monolayers and a study of their electrical properties, *Proc. Natl. Acad. Sci. U.S.A. 69*, 3561−3566.

27. Rance, M., Sorensen, O. W., Bodenhausen, G., Wagner, G., Ernst, R. R., and Wuthrich, K. (1983) Improved spectral resolution in cosy ^{1}H NMR spectra of proteins via double quantum filtering, *Biochem. Biophys. Res. Commun. 117*, 479−485.

28. Derome, A. E., and Williamson, M. P. (1990) Rapid-pulsing artifacts in doube-quantum-filtered COSY, *J. Magn. Reson. 88*, 177−185.

29. Bax, A., and Davis, G. D. (1985) MLEV-17-based two-dimensional homonuclear magnetization transfer spectroscopy, *J. Magn. Reson. 65*, 355−360.

30. Rance, M. (1987) Improved techniques for homonuclear rotating-frame and isotropic mixing experiments, *J. Magn. Reson. 74*, 557−564.

31. Macura, S., Huang, Y., Suter, D., and Ernst, R. R. (1981) Two-dimensional chemical exchange and cross-relaxation spectroscopy of coupled nuclear spins. *J. Magn. Reson. 43*, 259−281.

32. Marion, D., Ikura, M., Tschudin, R., and Bax, A. (1989) Rapid recording of 2D NMR spectra without phase cycling. Application to the study of hydrogen exchange in proteins. *J. Magn. Reson. 85*, 393−399.

33. Piotto, M., Saudek, V., and Sklenar, V. (1992) Gradient-tailored excitation for single-quantum NMR spectroscopy of aqueous solutions, *J. Biomol. NMR 2*, 661−665.

34. Wüthrich, K. (1986) *NMR of Proteins and Nucleic Acids*, John Wiley & Sons, New York.

35. Guntert, P., Mumenthaler, C., and Wuthrich, K. (1997) Torsion angle dynamics for NMR structure calculation with the new program DYANA, *J. Mol. Biol. 273*, 283−298.

36. Laskowski, R. A., Rullmannn, J. A., MacArthur, M. W., Kaptein, R., and Thornton, J. M. (1996) AQUA and PROCHECK-NMR: Programs for checking the quality of protein structures solved by NMR, *J. Biomol. NMR 8*, 477−486.

37. Frishman, D., and Argos, P. (1995) Knowledge-based protein secondary structure assignment, *Proteins 23*, 566−579.

38. Hall, J. E., Vodyanoy, I., Balasubramanian, T. M., and Marshall, G. R. (1984) Alamethicin. A rich model for channel behavior, *Biophys. J. 45*, 233−247.

39. Wishart, D. S., Bigam, C. G., Holm, A., Hodges, R. S., and Sykes, B. D. (1995) ^{1}H, ^{13}C and ^{15}N random coil NMR chemical shifts of the common amino acids. I. Investigations of nearest-neighbor effects, *J. Biomol. NMR 5*, 67−81.

40. Wishart, D. S., and Case, D. A. (2001) Use of chemical shifts in macromolecular structure determination, *Methods Enzymol. 338*, 3−34.

41. Fregeau Gallagher, N. L., Sailer, M., Niemczura, W. P., Nakashima, T. T., Stiles, M. E., and Vederas, J. C. (1997) Three-dimensional structure of leucocin A in trifluoroethanol and dodecylphosphocholine micelles: Spatial location of residues critical for biological activity in type IIa bacteriocins from lactic acid bacteria, *Biochemistry 36*, 15062−15072.

42. Sharon, M., Oren, Z., Shai, Y., and Anglister, J. (1999) 2D-NMR and ATR-FTIR study of the structure of a cell-selective diastereomer of melittin and its orientation in phospholipids, *Biochemistry 38*, 15305−15316.

43. Park, K., Oh, D., Shin, S. Y., Hahm, K. S., and Kim, Y. (2002) Structural studies of porcine myeloid antibacterial peptide PMAP-23 and its analogues in DPC micelles by NMR spectroscopy, *Biochem. Biophys. Res. Commun. 290*, 204−212.

44. Shenkarev, Z. O., Balashova, T. A., Efremov, R. G., Yakimenko, Z. A., Ovchinnikova, T. V., Raap, J., and Arseniev, A. S. (2002) Spatial structure of zervamicin IIB bound to DPC micelles: Implications for voltage-gating, *Biophys. J. 82*, 762−771.

45. Uteng, M., Hauge, H. H., Markwick, P. R., Fimland, G., Mantzilas, D., Nissen-Meyer, J., and Muhle-Goll, C. (2003) Three-dimensional structure in lipid micelles of the pediocin-like antimicrobial peptide sakacin P and a sakacin P variant that is structurally stabilized by an inserted C-terminal disulfide bridge, *Biochemistry 42*, 11417−11426.

46. Syvitski, R. T., Burton, I., Mattatall, N. R., Douglas, S. E., and Jakeman, D. L. (2005) Structural characterization of the antimicrobial peptide pleurocidin from winter flounder, *Biochemistry 44*, 7282−7293.

47. Yu, K., Park, K., Kang, S. W., Shin, S. Y., Hahm, K. S., and Kim, Y. (2002) Solution structure of a cathelicidin-derived antimicrobial peptide, CRAMP as determined by NMR spectroscopy, *J. Pept. Res. 60*, 1−9.

48. Tack, B. F., Sawai, M. V., Kearney, W. R., Robertson, A. D., Sherman, M. A., Wang, W., Hong, T., Boo, L. M., Wu, H., Waring, A. J., and Lehrer, R. I. (2002) SMAP-29 has two LPS-binding sites and a central hinge, *Eur. J. Biochem. 269*, 1181−1189.

49. Vignal, E., Chavanieu, A., Roch, P., Chiche, L., Grassy, G., Calas, B., and Aumelas, A. (1998) Solution structure of the antimicrobial peptide ranalexin and a study of its interaction with perdeuterated dodecylphosphocholine micelles, *Eur. J. Biochem. 253*, 221−228.

50. Chekmenev, E. Y., Vollmar, B. S., Forseth, K. T., Manion, M. N., Jones, S. M., Wagner, T. J., Endicott, R. M., Kyriss, B. P., Homem, L. M., Pate, M., He, J., Raines, J., Gor'kov, P. L., Brey, W. W., Mitchell, D. J., Auman, A. J., Ellard-Ivey, M. J., Blazyk, J., and Cotten, M. (2006) Investigating molecular recognition and biological function at interfaces using piscidins, antimicrobial peptides from fish, *Biochim. Biophys Acta 1758*, 1359−1372.

51. Sforca, M. L., Machado, A., Figueredo, R. C., Oyama, S., Jr., Silva, F. D., Miranda, A., Daffre, S., Miranda, M. T., Spisni, A., and Pertinhez, T. A. (2005) The micelle-bound structure of an antimicrobial peptide derived from the α-chain of bovine hemoglobin isolated from the tick *Boophilus microplus*, *Biochemistry 44*, 6440−6451.

52. Taylor, R. J., and de Levie, R. (1991) "Reversed" alamethicin conductance in lipid bilayers, *Biophys. J. 59*, 873−879.

53. Duclohier, H., Molle, G., and Spach, G. (1989) Antimicrobial peptide magainin I from *Xenopus* skin forms anion-permeable channels in planar lipid bilayers, *Biophys. J. 56*, 1017−1021.

54. Saint, N., Cadiou, H., Bessin, Y., and Molle, G. (2002) Antibacterial peptide pleurocidin forms ion channels in planar lipid bilayers, *Biochim. Biophys. Acta 1564*, 359−364.

55. Uematsu, N., and Matsuzaki, K. (2000) Polar angle as a determinant of amphipathic α-helix-lipid interactions: A model peptide study, *Biophys. J. 79*, 2075−2083.

56. Vogt, B., Ducarme, P., Schinzel, S., Brasseur, R., and Bechinger, B. (2000) The topology of lysine-containing amphipathic peptides in bilayers by circular dichroism, solid-state NMR, and molecular modeling, *Biophys. J. 79*, 2644−2656.

57. Kraulis, P. J. (1991) MOLSCRIPT. A program to produce both detailed and schematic plot of protein structures. *J. Appl. Crystallogr. 24*, 946−950.

BI0620297